
Federated Causal Discovery from Interventions

Amin Abyaneh¹ Nino Scherrer² Patrick Schwab³ Stefan Bauer⁴ Bernhard Schölkopf⁵ Arash Mehrjou^{3,5,2}

¹Electrical and Computer Engineering Dept., McGill University, Montréal, Canada

²ETH Zürich, Zürich, Switzerland

³GlaxoSmithKline, Artificial Intelligence and Machine Learning, Zug, Switzerland

⁴TU Munich & Helmholtz AI, Munich, Germany

⁵Max Planck Institute for Intelligent Systems, Tübingen, Germany

Abstract

Causal discovery serves a pivotal role in mitigating model uncertainty through recovering the underlying causal mechanisms among variables. In many practical domains, such as healthcare, access to the data gathered by individual entities is limited, primarily for privacy and regulatory constraints. However, the majority of existing causal discovery methods require the data to be available in a centralized location. In response, researchers have introduced *federated* causal discovery. While previous federated methods consider distributed observational data, the integration of *interventional data* remains largely unexplored. We propose FedCDI^a, a federated framework for inferring causal structures from distributed data containing interventional samples. In line with the federated learning framework, FedCDI improves privacy by exchanging belief updates rather than raw samples. Additionally, it introduces a novel intervention-aware method for aggregating individual updates. We analyze scenarios with shared or disjoint intervened covariates, and mitigate the adverse effects of interventional data heterogeneity. Performance and scalability of FedCDI is rigorously tested across a variety of synthetic and real-world graphs.

^agithub.com/aminabyaneh/fed-cdi

1 INTRODUCTION

The fundamental and challenging problem of discovering cause-effect relationships has long captivated the attention of statisticians [Pearl, 2009]. Recovering causal structures from data provides valuable insights for decision-making under uncertainty, as precise causal models of covariates empower exploration of potential outcomes of interventions

and hence, mitigate the unpredictability caused by external factors [Bhattacharya et al., 2020, Vowels et al., 2022].

Conventional causal discovery approaches mainly rely on centralized data [Wang et al., 2017, Zheng et al., 2018, Ke et al., 2019]. However, when dealing with sensitive information, such as patients’ medical records, preserving privacy is essential and protected by strict regulations. As a result, such sensitive data remains *confidential* and *distributed* across multiple entities. Therefore, researchers have turned to federated causal discovery (FCD) [Li et al., 2020] to discover causal structures in decentralized settings.

Previous FCD efforts are either limited to data generated from a linear underlying causal mechanism [Ye et al., 2022, Huang et al., 2023, Mian et al., 2023b] or restricted to homogeneous data [Ye et al., 2022, Ng and Zhang, 2022]. Most notably, these methods are *merely oriented towards discovery from observational data*, gathered passively without perturbing the system. This exclusive reliance on observational samples confines the identified structures to Markov equivalence classes [Yang et al., 2018, Spirtes and Zhang, 2016] and significantly elevates model uncertainty [Jesson et al., 2020]. Utilizing interventional data, collected by applying targeted perturbations on the system [Hyttinen et al., 2013, Addanki et al., 2020], alleviates these limitations through enhancing identifiability [Wang et al., 2017, Brouillard et al., 2020, Ke et al., 2019, Tigas et al., 2022].

To address the absence of interventional data in federated settings, we present FedCDI: a federated causal discovery method relying on interventions. FedCDI learns a global causal structure from a federation of clients (entities), without direct access to their local data. To this end, clients adopt a neural causal discovery method, such as Lippe et al. [2021], to acquire a belief about the causal structure of their local data. These local findings are then aggregated on a server while conforming to the following two criteria: (1) clients exert a more substantial influence on the aggregated belief based on the quality of their interventional samples, and (2) data samples are not exchanged among clients or

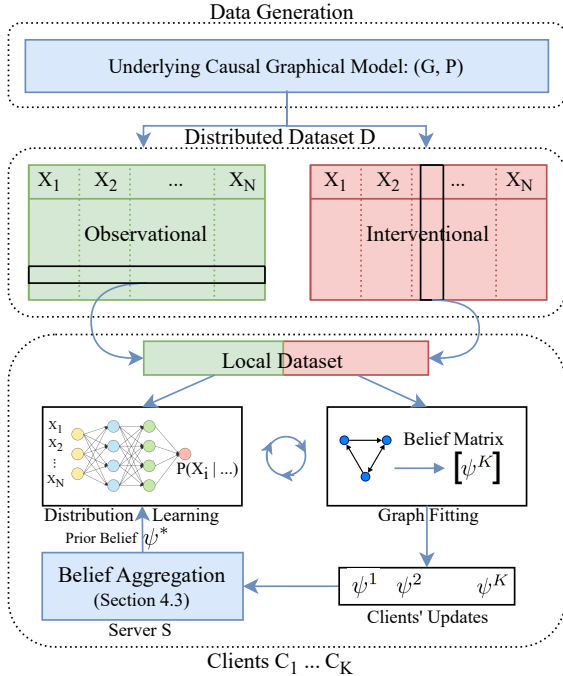


Figure 1: Overview of FedCDI, including the distributed dataset and local learning process. We only depict a single client, as the rest perform similar operations.

transmitted to the server. Instead, adhering to the federated learning paradigm, only belief updates are transmitted to the server during the aggregation process. An overview of FedCDI is presented in Figure 1.

Conforming to the mentioned criteria, FedCDI effectively aggregates clients’ updates based on the reliability of their local data. Owing to our novel knowledge aggregation method, clients’ contributions are rated by the extent of their access to interventional samples and the location of interventions in the causal structure. Therefore, a client provides a stronger contribution to the existence of a cause-effect relationship in the vicinity of its intervened covariates. Moreover, our approach poses few restrictive assumptions about the data generation mechanism, and endures a certain level of heterogeneity in interventional data. We empirically demonstrate that FedCDI performs similar to the centralized approaches, and outperforms FCD methods, when applied to data from synthetic and real-world causal structures.

2 RELATED WORK

Attempts to discover causal structures from distributed data precede the rise of federated learning. However, such distributed methods typically operate for a single round with no iterative improvement, and the majority decides the discovered DAG. For example, Gou et al. [2007] propose a two-step approach: obtaining a local Bayesian network, and

utilizing conditional independence tests to consolidate local updates. Moreover, Na and Yang [2010] develop a voting-based approach where the final structure is determined by most frequent patterns among local DAGs.

More recently, there has been a surge in FCD methods. FedDAG [Gao et al., 2021] is one of the first where at each round, clients learn an adjacency matrix to estimate the DAG and neural representation to approximate causal mechanisms. Ng and Zhang [2022] employ ADMM [Boyd et al., 2011] and apply a centralized optimization proposed by Zheng et al. [2018], to a federated setting. DARLS [Ye et al., 2022] is another method that counts on generalized linear models and distributed optimization to find an optimal DAG without violating clients’ privacy. Authors of PERI [Mian et al., 2023a] avoid the exchange of model parameters through regret-based aggregation to address privacy violations in previous methods, and Wang et al. [2023] extend conditional independence test to enable FCD with data heterogeneity.

Nevertheless, existing FCD methods face serious limitations, such as confinement to linear causal mechanisms or restricted to homogeneous data [Ng and Zhang, 2022, Mian et al., 2023b, Ye et al., 2022]. Notably, to the best of our knowledge, none of these methods, harness the valuable insights offered by interventional data. This underscores a *critical gap* between current FCD approaches, and the literature of DAG discovery based on interventions [Hauser and Bühlmann, 2015, Wang et al., 2017, Ke et al., 2019, Brouillard et al., 2020]. Although interventional data is more expensive to collect, researchers demonstrate that efficient utilization of such data significantly alleviates the identifiability challenge [Tigas et al., 2022].

Lastly, in this work, we build on DAG discovery methods based on continuous optimization. Unlike score-based methods [Hauser and Bühlmann, 2012], this class of algorithms avoids the combinatorial greedy search over DAGs through gradient-based optimization. DAGs with NO TEARS [Zheng et al., 2018, Yu et al., 2019] is considered the first to reformulate the greedy search as a continuous optimization problem [Vowels et al., 2022]. SDI [Ke et al., 2019], DCDI [Brouillard et al., 2020], and ENCO [Lippe et al., 2021] are introduced more recently as neural DAG discovery techniques to leverage interventional samples on top of regular observational data. Among the neural frameworks, ENCO [Lippe et al., 2021] presents a reliable and efficient DAG discovery method which formulates the graph search as optimization of independent edge likelihoods, while remaining scalable to large feature spaces.

3 BACKGROUND AND PROBLEM SETUP

Causal graphical models (CGM) provide mathematical abstraction to quantitatively describe causal relations be-

tween random variables. A CGM is a pair (G, P) , where $G = (X, E)$ is a *directed acyclic graph* (DAG), and P is a distribution faithful to G [Spirtes, 2010]. Within G , each node, $X_i \in X \forall i \in \{1, \dots, N\}$, represents a random variable, and a directed edge, $X_i \rightarrow X_j$, denotes the existence of a cause-effect relationship from X_i to X_j [Pearl, 2009]. We denote the adjacency matrix of G by $adj(G)_{N \times N}$.

Assumption 3.1 (*Causal Sufficiency*) *We assume causal sufficiency of the CGM, i.e., all common causes of variables are included and observable.*

An *intervention* on a random variable X is an applied perturbation on the system, such that it overrides the natural values of X that affects its probability distribution and (possibly) alters the DAG. We call the gathered data from an unperturbed system *observational*, $D_{\mathcal{O}}$, and we use the term *interventional*, $D_{\mathcal{I}}$, when the data is gathered from the perturbed system. The collection of these two datasets is denoted by $D := \{D_{\mathcal{O}}, D_{\mathcal{I}}\}$, that is a centralized dataset generated by unperturbed and perturbed CGM described by (G, P) .

Assumption 3.2 (*Perfect Interventions*). *Interventions in $D_{\mathcal{I}}$ are perfect, that is, $p_{\mathcal{I}}(X_i | Pa(X_i)) = p_{\mathcal{I}}(X_i)$, where $p_{\mathcal{I}}$ is the distribution of intervened X_i , and $Pa(X)$ denotes the parent variables of X within the DAG.*

Assumption 3.3 (*Stochastic and Known Interventions*). *Interventions are not designed to set the variable to a fixed value, and the intervened variable is known.*

Our proposed federated setup consists of a central node acting as a server and K other nodes as clients. We denote the server with S and the clients with, $C_k, \forall k \in \{1, \dots, K\}$. Each client is an independent processing unit, and can only communicate with the server. The centralized dataset D is distributed among the clients, where each client C_k has access to a (not necessarily disjoint) subset of D , called $D^k := \{D_{\mathcal{O}}^k, D_{\mathcal{I}}^k\}$. To utilize the entire dataset for structure discovery, we assume these subsets to span the entire D , such that $D = \bigcup_{k=1}^K D^k$.

Any dataset can be distributed either horizontally or vertically. Horizontal distribution leads to clients having access to the entire set of features, but only a fraction of samples. A vertical split, however, provides access to only a subset of features in the original centralized data. We consider a horizontal (homogeneous) split for $D_{\mathcal{O}}$ and vertical (heterogeneous) distribution of $D_{\mathcal{I}}$. Therefore, we assume that clients are aware of all the dataset features, but might not have access to interventional data corresponding to each node, X_i . The accessible set of intervened variables for each client, C_k , is represented by $X_{\mathcal{I}}^k \subset X$.

Assumption 3.4 (*Knowledge of Intervened Covariates*). *The information about $X_{\mathcal{I}}^k$, that is, the intervened covariates for C_k , is known to the server S .*

Note that unlike existing methods, we do not pose any restrictions on linearity or noise distribution of the CGM.

Problem statement. Within the described federated setting, we focus on recovering the underlying causal DAG, G , rather than the probability distribution, P , while enforcing a strict restriction on direct exchange of D^k samples either between two arbitrary clients, C_i and C_j , or to the server, S .

4 FEDERATED CAUSAL DISCOVERY FROM INTERVENTIONS

Following the federated learning paradigm, clients in Fed-CDI collaborate through a two-phase iterative process:

1. Local discovery (Section 4.1): Each client applies a local causal discovery method (LCDM) to yield a *prior belief* about G while incorporating an existing belief. Therefore, clients, C_k , securely share their belief with the server and not data samples or model parameters.
2. Global aggregation (Section 4.3): The server employs an aggregation method to find the updated belief from a collection of clients' communicated beliefs. Then, the server broadcasts the *aggregated belief* back to all clients, which they utilize to guide their local optimization in the next round.

We start with the first step in Section 4.1 by discussing the nature of the prior belief and LCDMs. In Section 4.2, we assume a horizontal distribution of $D_{\mathcal{I}}$, that is, every client has access to the same set of interventions. Yet, assuming identical intervened covariates is a naive assumption for real-world scenarios, where clients oftentimes hold interventional data on various covariates. Hence, in Section 4.3, we propose a proximity-based belief aggregation applicable to clients with non-identical sets of intervened variables, i.e., vertical distribution of $D_{\mathcal{I}}$. This simulates a level of heterogeneity between clients in interventional data, since the underlying data distributions are different across clients.

4.1 LOCAL DISCOVERY OF PRIOR BELIEFS

The goal in this stage is for each client to infer a belief about the global DAG. To this end, clients apply an LCDM to their local datasets, D^k . We design the LCDM to produce and later incorporate prior knowledge about the structure, and favor this knowledge when uncertain about the existence of any $X_i \rightarrow X_j \in E$. We define clients' beliefs with matrices of the same dimensions as $adj(G)$.

Definition 4.1 (*Belief Matrix*) *Let $\psi \in \mathbb{R}^{N \times N}$ be the matrix with elements ψ_{ij} , where ψ_{ij} is the parameter of an independent Bernoulli distribution, i.e., $Ber(\psi_{ij}) \forall i, j$. We call ψ the belief matrix, and each element, ψ_{ij} , corresponds to the existence probability of $X_i \rightarrow X_j$, i.e.,*

$P(X_i \rightarrow X_j) \sim \text{Ber}(\mathcal{B}_{i,j})$. The matrix ψ yields an adjacency matrix through an element-wise binary step function.

To learn ψ , we opt for neural LCDMs that learn similar belief matrices through continuous-optimization. For instance, ENCO [Lippe et al., 2021] uses $\gamma, \theta \in \mathbb{R}^{N \times N}$ matrices to represent the existence and orientation of edges in a graph, respectively. This formulation is not unique to ENCO and other methods, such as SDI [Ke et al., 2019] and DCDI [Brouillard et al., 2020] use similar belief matrices. We predominantly view ENCO as the preferred choice for clients' LCDM due to its efficient implementation and scalability.

The LCDM needs to consider the updated belief from the server into its local optimization. We achieve this by directly initializing the LCDM belief matrices, (γ, θ) in the case of ENCO, by sampling from Bernoulli distributions with ψ parameters, and enforcing this knowledge as a Lagrangian on LCDM's internal loss. To implement this, we take note that ENCO alternates between *distribution fitting* and *graph fitting* stages. Distribution fitting trains a neural network f_{ϕ_i} to model X_i 's conditional data distribution, $p(X_i | \mathbf{X}_{-i})$, on observational data. Then, the graph fitting stage learns γ and θ matrices by minimizing:

$$\mathcal{L} = \mathbb{E}_{\hat{I} \sim p_I(I)} \mathbb{E}_{\tilde{p}_i(X)} \mathbb{E}_{p_{\gamma, \theta}(\zeta)} \left[\sum_{i=1}^N \mathcal{L}_{\zeta}(X_i) \right] + \lambda_{\text{sparse}} \sum_{i=1}^N \sum_{j=1}^N \sigma(\gamma_{ij}) \cdot \sigma(\theta_{ij}), \quad (1)$$

where $p_I(I)$ and $\tilde{p}_i(X)$ represent interventional data distribution and $p_{\gamma, \theta}(\zeta)$ is the distribution over adjacency matrices with $\zeta_{ij} \sim \text{Ber}(\sigma(\gamma_{ij})\sigma(\theta_{ij}))$. Note that σ is the sigmoid function. Moreover, $\mathcal{L}_{\zeta}(X_i) = -\log f_{\phi_i}(X_i; \zeta_{\cdot, i} \odot X_{-i})$, that is the negative log-likelihood estimate of the variable X_i with the distribution learned from observational data. The last term is for sparsity regularization¹. We integrate an extra differentiable loss term to consider the prior belief in Equation (1), yielding $\tilde{\mathcal{L}} = \mathcal{L} + \lambda_{\text{prior}} \mathcal{L}_{\psi}$, and define the belief loss as,

$$\mathcal{L}_{\psi} = -\mathbb{E}_{i,j} [\zeta_{ij} \log(\psi_{ij}) + (1 - \zeta_{ij}) \log(1 - \psi_{ij})], \quad (2)$$

where the log loss measures the agreement between the observed values in ζ and the probabilities represented by ψ . Lower values of the log loss indicate a better agreement between ζ and ψ , encouraging the optimizer to find solutions that align with the prior belief. Hence, the optimization process of LCDM is guided by the belief, especially when facing uncertainty about the existence of an arbitrary edge, $X_i \rightarrow X_j$. Such uncertainties may arise when $D_{\mathcal{I}}^k$ lacks intervened covariates influencing the edge, $X_i \rightarrow X_j$.

¹Details of the optimization process and its tractability are provided in Lippe et al. [2021].

Algorithm 1 Federated causal discovery from observational and interventional data. The algorithm for proximity-based aggregation method is provided in Algorithm 2.

Data: $D := \{D_{\mathcal{O}}, D_{\mathcal{I}}\}; T := \text{n_rounds} \in \mathbb{N}$
Return: $\tilde{G} :=$ discovered causal DAG
for T iterations **or** convergence **do** ▷ Federated rounds
 for $k = 1$ **to** K **do**
 $\psi^k \leftarrow$ local_causal_discovery_method(D^k, ψ)
 ▷ Parallel local learning (section 4.1)
 end for
 $\psi \leftarrow$ proximity_based_aggregation($\psi, \{\psi^1, \dots, \psi^k\}$)
 ▷ Model aggregation stage (section 4.3)
end for
 $\text{adj}(\tilde{G}) \leftarrow$ binary_step($\psi^*, \text{threshold} = 0.5$)

4.2 NAIVE BELIEF AGGREGATION

In a naive scenario, we assume $X_{\mathcal{I}}^k = X, \forall k \in \{1, \dots, K\}$. Let ψ^k be the prior belief obtained by each client, after transmission of ψ^k to the server, the aggregated belief is calculated by a weighted average over ψ^k matrices through,

$$\psi^* = \sum_k w_k \psi^k, w_k = \frac{\text{size}(D^k)}{\text{size}(D)}, \forall k \in \{1, \dots, K\}, \quad (3)$$

where ψ_{ij}^* is the aggregated belief. Because $w_1 + w_2 + \dots + w_K = 1$, each element of the weighted sum ψ_{ij}^* represents the parameter of a Bernoulli distribution. However, without access to same intervened covariates across clients' interventional dataset, this method fails to take client's expertise into account. Intuitively, a client with access to direct interventions on X_i is more confident about the edge probability of $X_i \rightarrow X_j$ than a client without such knowledge. Nonetheless, this approach can serve as a naive baseline designed for homogeneous D^k distributions, filling the void of FCD methods that harness interventional data.

4.3 PROXIMITY-BASED BELIEF AGGREGATION

We know that D^k , contains interventions on the set of variables indicated by $X_{C_k}^{\mathcal{I}}$. After applying LCDM to the local data, ψ_{ij}^k is the posterior probability of $X_i \rightarrow X_j$'s existence, calculated by the client C_k . The challenge is to come up with an aggregation method for posteriors, $\psi_{ij}^k \forall k \in \{1, \dots, K\}$, while considering the clients' knowledge of applied interventions.

Proposition 4.2 Consider $X_i, X_j \in X$ to be two arbitrary variables in G . Then, for a client C_k admitting an intervened variable, $X_s \in X_{\mathcal{I}}^k$, the reliability of ψ_{ij}^k , denoted by $r_{ij}^k \in [0, 1]$, is higher if $X_i \rightarrow X_j$ belongs to a path in G descending from X_s .

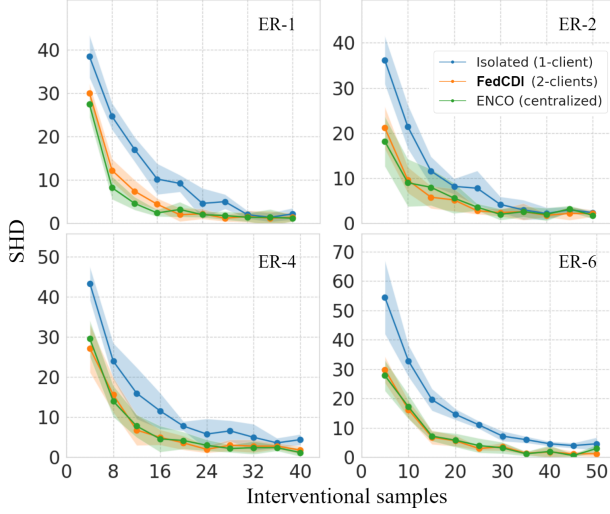


Figure 2: FedCDI is rigorously compared against a centralized approach and an isolated client, taking for various interventional data sizes. Within the centralized approach, the entire dataset is available, while in both FedCDI and the isolated client, each client is limited to only half of D distributed horizontally.

Sketch of the proof. Note that if the described path exists, then every variable X_i in the described path is a descendant of X_s . The proof is straightforward through causal factorization [Spirtes, 2010],

$$P(X) = \prod_{i=1}^N P(X_i | \text{Pa}(X_i)), \quad (4)$$

$$P(X_i, X_j) = P(X_j | \text{Pa}(X_j)) \cdot P(X_i | \text{Pa}(X_i)). \quad (5)$$

Then, assuming an intervention on X_s and the truncated factorization formula (causal factorization with applied intervention [Pearl, 2009]), we write Equation (4) for $X_i \rightarrow X_j$,

$$P(X \setminus X_s | \text{do}(X_s = x)) = \prod_{i | X_i \neq X_s} P(X_i | \text{Pa}(X_i)) \Big|_x,$$

$$P(X_i, X_j | \text{do}(X_s = x)) = \prod_{t \in \{i, j\}} P(X_t | \text{Pa}(X_t)) \Big|_x,$$

where it becomes clear that altering X_s 's distribution directly affects its descendants. \square

In order to find r_{ij}^k for each client, we inject hypothetical mass m_s^k to the node X_s and let the mass flow in the DAG without its magnitude being divided by the fan-out of each node. When passing through any edge $X_q \rightarrow X_p$ on the way, the mass value is multiplied by ψ_{qp} where ψ_{qp} is the current aggregated belief in the network. The new mass then continues to flow in the graph in the same manner. For instance, the reliability score of the edge $X_s \rightarrow X_p$ is $\psi_{sp}^k m_s^k$. The score becomes $\psi_{sp}^k \psi_{pq}^k m_s^k$ for $X_p \rightarrow X_q$.

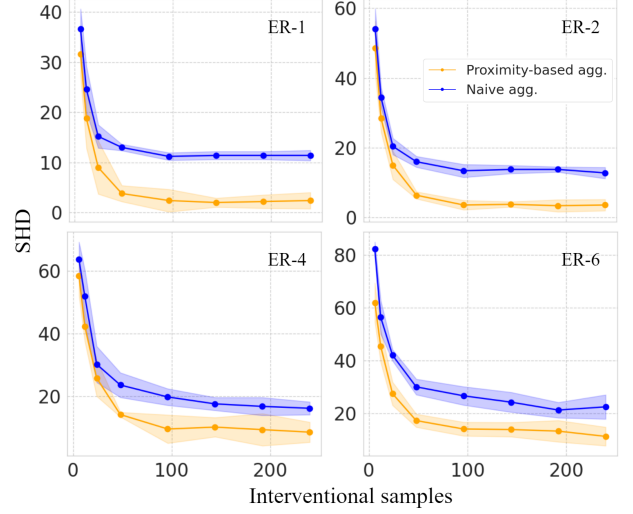


Figure 3: We apply the proximity-based and naive aggregation methods to vertically distributed $D_{\mathcal{I}}$. Each curve corresponds to a 5-client setup, where clients have access to disjoint and covering subsets of vertically distributed interventional dataset, i.e., local datasets contain interventional samples on only 4 out of 20 dataset features.

Should different mass values reach the same node from multiple paths, we pick the maximum regardless of the source variables. After a sufficient number of steps, the mass flows through the entire DAG.

All clients perform the same process only once at each round, based on the latest aggregated belief, ψ . Let the mass passing through an edge be the reliability score for that edge. The process yields a set of reliability scores, $\{r_{ij}^1, r_{ij}^2, \dots, r_{ij}^K\}$, assigned to each edge $X_i \rightarrow X_j$. We cannot directly use r_{ij}^k values for aggregating the local beliefs $\{\psi_{ij}^1, \psi_{ij}^2, \dots, \psi_{ij}^K\}$ as $\sum_k r_{ij}^k \neq 1$. To turn r_{ij}^k values into probabilities, we apply a softmax function and write the new aggregated belief, $\forall k \in \{1, \dots, K\}$,

$$\psi_{ij}^* = \sum_{k \in [K]} \hat{r}_{ij}^k \psi_{ij}^k, \quad \hat{r}_{ij}^k = \frac{e^{\beta r_{ij}^k}}{\sum_{k \in [K]} e^{\beta r_{ij}^k}}, \quad (6)$$

where ψ_{ij}^* is the aggregated belief and $\beta > 0$ is the temperature parameter of the softmax function. The rate parameter β controls the sensitivity of the distribution of \hat{r}_{ij}^k to the difference of the reliability scores calculated by different clients. This procedure has the following parameters:

- m_i^k , $\forall i \in \{i | X_i \in X_{\mathcal{I}}^k\}$, the initial mass of C_k . We set this parameter proportionate to the number of interventional samples for X_i available in D^k .
- β , the softmax temperature, optimized by a grid search over a computationally feasible set.

Algorithm 1 presents FedCDI and our novel proximity-

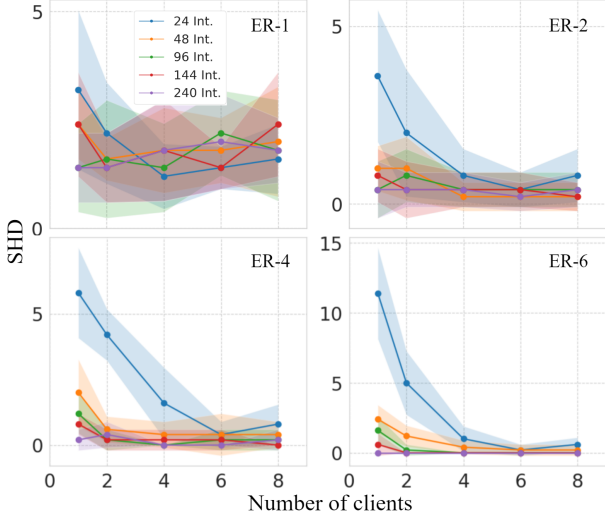


Figure 4: Effect of additional clients participating in FedCDI for different $D_{\mathcal{I}}$ sizes. The discovered DAG is more accurate where $size(D_{\mathcal{I}})$ increases with the addition of new clients.

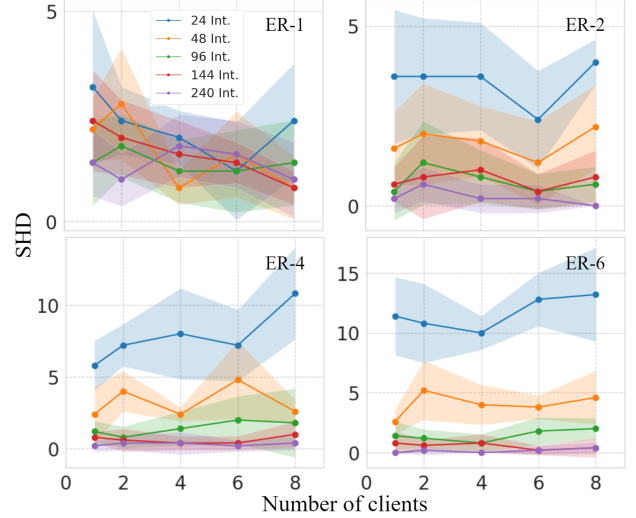
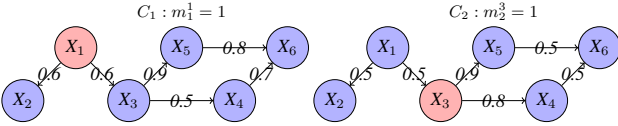


Figure 5: FedCDI manages to sustain the knowledge when the fixed-size $D_{\mathcal{I}}$ is further divided by the increase in number of clients, as opposed to Figure 4.

based aggregation. We conclude this section by providing a toy example to illustrate the proposed belief aggregation.

Example 4.2.1 Let's consider a 2-client setup. C_1 has interventional samples on X_1 (left), whereas C_2 holds interventional data on X_3 (right). We assume the clients have an equal number of samples, $m_1^1 = m_2^3 = 1$, and $\beta = 2$ and ψ_{ij} acquired from last aggregation are written on the edges. Edges with $\psi_{ij} < 0.5$ are omitted for simplicity.



The flow of mass for C_1 and C_2 yields:

$$r_{5,6}^1 = 0.6 \cdot 0.9 \cdot 0.8 \cdot m_1^1 = 0.432,$$

$$r_{5,6}^2 = 0.9 \cdot 0.5 \cdot m_2^3 = 0.540 \Rightarrow R_{5,6} = \{0.432, 0.540\}.$$

Then, the final reliability score of C_1 and C_2 for $X_5 \rightarrow X_6$ is calculated by:

$$\hat{r}_{5,6}^1 = \frac{e^{(2 \times 0.432)}}{e^{(2 \times 0.432)} + e^{(2 \times 0.540)}} \approx 0.446,$$

$$\hat{r}_{5,6}^2 = \frac{e^{(2 \times 0.540)}}{e^{(2 \times 0.540)} + e^{(2 \times 0.432)}} \approx 0.554.$$

5 EXPERIMENTS

To empirically showcase the efficacy of FedCDI, we conduct a thorough evaluation by comparing its results against both

a centralized setting and non-collaborating clients. Additionally, we scrutinize naive averaging-based and proximity-based aggregation methods discussed earlier, providing specific insights into the limitations of the former when confronted with vertical data distributions. Finally, we conclude our assessment with scalability experiments and a comparative analysis of FedCDI against selected baselines in the literature on both real-world and synthetic graphs.

5.1 EXPERIMENT SETUP

DAGs. For *synthetic* data, we employ the random Erdős-Rényi (ER) model to pick experimental DAGs of size $d = 20$, where each edge is added with an independent pre-determined probability from the others [Erdős and Rényi, 2011]. We experiment on data generated by $ER - n$ DAGs where $n \in \{1, 2, 4, 6\}$. According to the definition, the value of $n \cdot d$ is equal to the expected number of edges. For the *real-world* graphs in the last section, we turn to `bnlearn` package [Scutari, 2010], and pick Sachs [Sachs et al., 2005], Alarm [Beinlich et al., 1989], and Asia [Lauritzen and Spiegelhalter, 1988] graphs.

Dataset. The global dataset, D , is generated based on the previously sampled DAGs, and by employing the a synthetic data generation mechanism similar to Ke et al. [2019]. The process utilizes randomly initialized neural networks with two layers with categorical inputs to model the ground-truth conditional distributions. We sample categorical data with 10 categories in different sizes for both interventional and observational sets. For all experiments, the observational data is horizontally distributed among clients. However, a client may receive interventional samples for all intervened

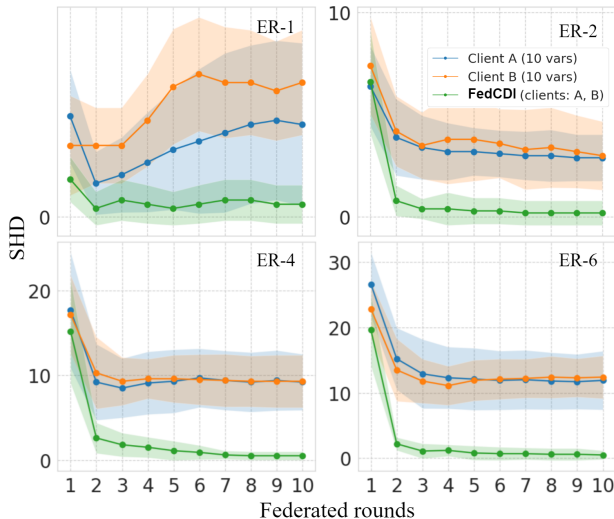


Figure 6: Non-collaborative clients A and B with access to vertical subsets of $D_{\mathcal{I}}$, and FedCDI where the same A and B clients now share their belief about the structure.

variables (horizontal) or only a subset of those variables (vertical). Further details about the data generation process appear on Appendix B. We also apply FedCDI to the data generated from structured graphs in Appendix A.

Evaluation. We compare the outcome of each setup to the ground truth by calculating the Structural Hamming Distance (SHD) between the two. Note that the outcome for FedCDI is calculated by applying a binary step function (threshold = 0.5) to the final belief matrix. We then run each experiment for 20 random seeds, and report the SHD average and confidence interval.

5.2 HORIZONTAL DATA DISTRIBUTION

We start with a scenario where both $D_{\mathcal{O}}$ and $D_{\mathcal{I}}$ are split horizontally. Figure 2 presents multiple experiments with our method while employing the proximity-based aggregation. The results clearly demonstrate that two collaborative clients outperform an isolated client. Moreover, it is evident that FedCDI discovers a DAG with the same precision as the centralized approach. Therefore, the belief aggregation step performs an effective aggregation of clients’ information without directly exchanging samples. Note that as the size of $D_{\mathcal{I}}$ increases in Figure 2, the results of the isolated client come closer to FedCDI, as each client now holds adequate samples to find the underlying DAG without collaboration.

5.3 VERTICAL DISTRIBUTION OF INTERVENTIONAL DATA

To highlight the critical role of interventional data in FCD, we vertically distribute $D_{\mathcal{I}}$, limiting clients’ interventional

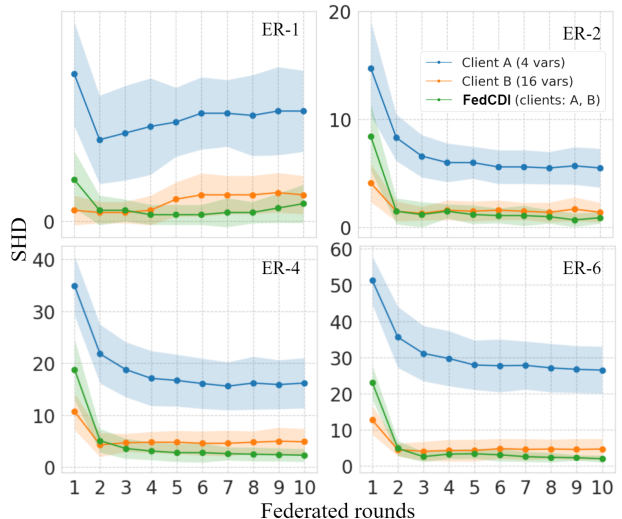


Figure 7: We further extend the setup in Figure 6 to demonstrate the way our aggregation method leverages the information received from clients with fewer intervened covariates.

samples to a subset of dataset covariates. Figure 3 compares naive averaging-based aggregation method to the more sophisticated proximity-based aggregation and suggests that naive averaging underperforms as it disregards clients’ unique access to interventions.

We further showcase the ability of proximity-based aggregation in Figure 6. Two isolated clients are compared against a 2-client federated setup, where the same two clients collaborate through FedCDI and yield superior results. Moreover, Figure 7 illustrates that a client with access to the majority of interventional data still benefits from collaborating with the less significant client. This is justified as FedCDI exploits the second client’s knowledge of interventional samples, which are critical to precise DAG discovery.

5.4 PERFORMANCE WITH MORE COLLABORATING CLIENTS

To assess the effect of increasing the number of clients, we performed two series of experiments. In Figure 4, new clients join FedCDI by bringing their own local dataset. Therefore, the size of $D_{\mathcal{I}}$ increases upon adding a new client, and more information becomes available in the network, while D^k have a fixed size. Then, we keep $size(D_{\mathcal{I}})$ constant in Figure 5, and then increase the number of clients. Each new client receives a share by joining the setup, leaving the others with fewer samples.

The results implicate that FedCDI experiences higher precision when clients with new information are added to the collaborative environment. Each client brings fresh samples, which in turn helps the aggregation stage to learn more accurate existence probabilities. However, even in the case of

Table 1: Comparison between FedCDI and baselines selected in Section 5.5 for **synthetic** ($ER - n$) and **real-world** (*Sachs*, *Alarm*, *Asia*) graphs. Results are averaged over 20 random seeds. The top two highest scores in each graph are bolded.

Data	Method	ER-1	ER-2	ER-4	ER-6	Sachs	Alarm	Asia
Centralized & Interventional	GIES	14.4 ± 2.1	46.9 ± 0.8	127.3 ± 1.6	168.8 ± 0.7	21.3 ± 4.3	43.2 ± 7.5	13.8 ± 3.1
	IGSP	11.8 ± 2.8	43.7 ± 0.7	118.5 ± 0.4	152.8 ± 0.1	14.4 ± 3.4	25.1 ± 1.4	12.6 ± 2.7
	DCDI	3.0 ± 1.1	24.3 ± 2.1	31.4 ± 8.6	43.0 ± 12.3	6.9 ± 1.2	36.8 ± 2.3	6.1 ± 1.6
	ENCO	1.9 ± 0.1	4.3 ± 0.1	5.7 ± 0.2	7.8 ± 0.3	0.5 ± 0.4	13.8 ± 2.5	2.0 ± 0.1
Federated & Observational	FedDAG	10.3 ± 1.9	14.2 ± 1.4	17.6 ± 0.7	24.5 ± 3.6	5.4 ± 1.0	11.2 ± 0.8	1.5 ± 0.6
	NOTEARS-ADMM	7.7 ± 3.0	15.8 ± 4.9	17.2 ± 2.4	21.1 ± 5.3	6.1 ± 2.2	8.2 ± 1.5	4.7 ± 1.2
Federated & Interventional	FedCDI (2-clients)	2.6 ± 0.6	3.9 ± 0.4	4.1 ± 0.1	5.5 ± 0.3	0.9 ± 0.3	19.8 ± 2.6	8.8 ± 2.5
	FedCDI (4-clients)	2.3 ± 0.4	3.3 ± 0.7	4.6 ± 0.6	5.7 ± 0.4	0.8 ± 0.5	8.0 ± 3.1	1.7 ± 0.4

$D_{\mathcal{I}}$'s further division by adding new clients, FedCDI maintains effective knowledge aggregation. The only breaking point happens when clients are left with so few samples, that even the LCDM itself fails to converge to a local graph (see convergence conditions in Lippe et al. [2021]).

5.5 BASELINES AND GENERALIZATION

We compare our setup against well-known DAG discovery methods which leverage both interventional and observational data. From the methods listed in Guo et al. [2020], we pick GIES [Hauser and Bühlmann, 2012], IGSP [Wang et al., 2017], and DCDI [Brouillard et al., 2020], apply them in a centralized manner to $\{D_{\mathcal{O}}, D_{\mathcal{I}}\}$, and report the results. We then apply FedDAG [Gao et al., 2021] and NOTEARS-ADMM [Ng and Zhang, 2022] to the same data, despite their sole reliance on observational samples. The dataset size is the same across all baselines, but samples are divided between clients in FedCDI, FedDAG, and NOTEARS-ADMM. The results indicate the capability of FedCDI in knowledge aggregation, considering that each client has access to less information compared to centralized approaches, yet still the setup as a whole manages to yield precise discoveries.

6 LIMITATIONS AND FUTURE WORK

Real-world data. Real-world causal discovery datasets lack the required interventional samples to enable FedCDI's capabilities. fMRI Hippocampus [Poldrack et al., 2015] is an example of datasets employed by federated DAG discovery methods which solely contain observational samples. Even though we use real-world graphs from bnlearn Scutari [2010], we are bound to generate the corresponding data same as previous work [Ke et al., 2019, Brouillard et al., 2020, Lippe et al., 2021] in the literature.

Client data limitation. We observed that if clients have a limited local dataset lower than a certain threshold, the resulting DAG becomes highly inaccurate. Though this phenomenon is intuitive, the threshold depends on the choice of LCDM and the underlying data generation processes. Future

work could propose a generic method to yield this threshold.

Computational complexity. Although running clients' LCDM in parallel potentially reduces the overall computational time compared to a centralized approach, it can pose a higher computational load depending on the nature of the learning method. For instance, if the computational cost of the LCDM is linear regarding data and the overheads are negligible, then the computational load remains the same as a centralized approach. On the other hand, having a large overhead aside from dataset size leads to higher computational load compared to centralized approaches.

Acyclicity. One must ensure that the adjacency matrix obtained after several rounds of aggregation is still a DAG. Pruning the adjacency matrix corresponding to the final estimation is one option. Yet, future work could integrate extra constraints in the aggregation process to ensure acyclicity.

7 CONCLUSION

We developed a novel approach to federated DAG discovery from distributed datasets, aiming to enhance client privacy by avoiding the sharing of local samples. Concentrating on interventional data, we successfully uncover the underlying causal structure with precision and effectively handle both homogeneous and heterogeneous distributions of interventional data. Through extensive experiments, we demonstrate the scalability and performance of FedCDI, and compare it to centralized and federated methods. Our use of a naive aggregation further highlights the advantage of considering clients' interventions. FedCDI empirical results underscore its superiority against compared to previous FCD methods.

8 REPRODUCIBILITY

FedCDI's source code (sites.google.com/view/fedcdi) is published, and the repository includes all the essential reproducibility instructions. To ease off reproducibility, the raw data can be downloaded, especially for experiments which require significant computational resources.

References

- Raghavendra Addanki, Shiva Kasiviswanathan, Andrew McGregor, and Cameron Musco. Efficient intervention design for causal discovery with latents. In *International Conference on Machine Learning*, pages 63–73. PMLR, 2020.
- Ingo A Beinlich, Henri Jacques Suermondt, R Martin Chavez, and Gregory F Cooper. The alarm monitoring system: A case study with two probabilistic inference techniques for belief networks. In *AIME 89*, pages 247–256. Springer, 1989.
- Rohit Bhattacharya, Daniel Malinsky, and Ilya Shpitser. Causal inference under interference and network uncertainty. In *Uncertainty in Artificial Intelligence*, pages 1028–1038. PMLR, 2020.
- Stephen Boyd, Neal Parikh, Eric Chu, Borja Peleato, Jonathan Eckstein, et al. Distributed optimization and statistical learning via the alternating direction method of multipliers. *Foundations and Trends® in Machine Learning*, 3(1):1–122, 2011.
- Philippe Brouillard, Sébastien Lachapelle, Alexandre Lacoste, Simon Lacoste-Julien, and Alexandre Drouin. Differentiable causal discovery from interventional data. *Advances in Neural Information Processing Systems*, 33: 21865–21877, 2020.
- Paul Erdős and Alfréd Rényi. On the evolution of random graphs. In *The structure and dynamics of networks*, pages 38–82. Princeton University Press, 2011.
- Erdun Gao, Junjia Chen, Li Shen, Tongliang Liu, Mingming Gong, and Howard Bondell. Feddag: Federated dag structure learning. *arXiv preprint arXiv:2112.03555*, 2021.
- Kui Xiang Gou, Gong Xiu Jun, and Zheng Zhao. Learning bayesian network structure from distributed homogeneous data. In *Eighth acis international conference on software engineering, artificial intelligence, networking, and parallel/distributed computing (snpd 2007)*, volume 3, pages 250–254. IEEE, 2007.
- Ruo Cheng Guo, Lu Cheng, Jundong Li, P Richard Hahn, and Huan Liu. A survey of learning causality with data: Problems and methods. *ACM Computing Surveys (CSUR)*, 53(4):1–37, 2020.
- Alain Hauser and Peter Bühlmann. Characterization and greedy learning of interventional markov equivalence classes of directed acyclic graphs. *The Journal of Machine Learning Research*, 13(1):2409–2464, 2012.
- Alain Hauser and Peter Bühlmann. Jointly interventional and observational data: estimation of interventional markov equivalence classes of directed acyclic graphs. *Journal of the Royal Statistical Society: Series B (Statistical Methodology)*, 77(1):291–318, 2015.
- Jianli Huang, Xianjie Guo, Kui Yu, Fuyuan Cao, and Jiye Liang. Towards privacy-aware causal structure learning in federated setting. *IEEE Transactions on Big Data*, 2023.
- Antti Hyttinen, Frederick Eberhardt, and Patrik O Hoyer. Experiment selection for causal discovery. *Journal of Machine Learning Research*, 14:3041–3071, 2013.
- Andrew Jesson, Sören Mindermann, Uri Shalit, and Yarin Gal. Identifying causal-effect inference failure with uncertainty-aware models. *Advances in Neural Information Processing Systems*, 33:11637–11649, 2020.
- Diviyani Kalainathan, Olivier Goudet, and Ritik Dutta. Causal discovery toolbox: Uncovering causal relationships in python. *The Journal of Machine Learning Research*, 21(1):1406–1410, 2020.
- Nan Rosemary Ke, Olexa Bilaniuk, Anirudh Goyal, Stefan Bauer, Hugo Larochelle, Bernhard Schölkopf, Michael C Mozer, Chris Pal, and Yoshua Bengio. Learning neural causal models from unknown interventions. *arXiv preprint arXiv:1910.01075*, 2019.
- Steffen L Lauritzen and David J Spiegelhalter. Local computations with probabilities on graphical structures and their application to expert systems. *Journal of the Royal Statistical Society: Series B (Methodological)*, 50(2):157–194, 1988.
- Tian Li, Anit Kumar Sahu, Ameet Talwalkar, and Virginia Smith. Federated learning: Challenges, methods, and future directions. *IEEE Signal Processing Magazine*, 37(3):50–60, 2020.
- Phillip Lippe, Taco Cohen, and Efstratios Gavves. Efficient neural causal discovery without acyclicity constraints. In *International Conference on Learning Representations*, 2021.
- Osman Mian, David Kaltenpoth, Michael Kamp, and Jilles Vreeken. Nothing but regrets—privacy-preserving federated causal discovery. In *International Conference on Artificial Intelligence and Statistics*, pages 8263–8278. PMLR, 2023a.
- Osman Mian, David Kaltenpoth, Michael Kamp, and Jilles Vreeken. Nothing but regrets—privacy-preserving federated causal discovery. In *International Conference on Artificial Intelligence and Statistics*, pages 8263–8278. PMLR, 2023b.
- Yongchan Na and Jihoon Yang. Distributed bayesian network structure learning. In *2010 IEEE International Symposium on Industrial Electronics*, pages 1607–1611. IEEE, 2010.

- Ignavier Ng and Kun Zhang. Towards federated bayesian network structure learning with continuous optimization. In *International Conference on Artificial Intelligence and Statistics*, pages 8095–8111. PMLR, 2022.
- Judea Pearl. *Causality*. Cambridge university press, 2009.
- Russell A Poldrack, Timothy O Laumann, Oluwasanmi Koyejo, Brenda Gregory, Ashleigh Hover, Mei-Yen Chen, Krzysztof J Gorgolewski, Jeffrey Luci, Sung Jun Joo, Ryan L Boyd, et al. Long-term neural and physiological phenotyping of a single human. *Nature communications*, 6(1):8885, 2015.
- Karen Sachs, Omar Perez, Dana Pe’er, Douglas A Luffenburger, and Garry P Nolan. Causal protein-signaling networks derived from multiparameter single-cell data. *Science*, 308(5721):523–529, 2005.
- Marco Scutari. Learning bayesian networks with the bnlearn R package. *Journal of Statistical Software*, 35(3):1–22, 2010. doi: 10.18637/jss.v035.i03.
- Peter Spirtes. Introduction to causal inference. *Journal of Machine Learning Research*, 11(5), 2010.
- Peter Spirtes and Kun Zhang. Causal discovery and inference: concepts and recent methodological advances. In *Applied informatics*, volume 3, pages 1–28. SpringerOpen, 2016.
- Panagiotis Tigas, Yashas Annadani, Andrew Jesson, Bernhard Schölkopf, Yarin Gal, and Stefan Bauer. Interventions, where and how? experimental design for causal models at scale. *Advances in Neural Information Processing Systems*, 35:24130–24143, 2022.
- Matthew J Vowels, Necati Cihan Camgoz, and Richard Bowden. D’ya like dags? a survey on structure learning and causal discovery. *ACM Computing Surveys*, 55(4):1–36, 2022.
- Yuhao Wang, Liam Solus, Karren Yang, and Caroline Uhler. Permutation-based causal inference algorithms with interventions. *Advances in Neural Information Processing Systems*, 30, 2017.
- Zhaoyu Wang, Pingchuan Ma, and Shuai Wang. Towards practical federated causal structure learning. *arXiv preprint arXiv:2306.09433*, 2023.
- Karren Yang, Abigail Katcoff, and Caroline Uhler. Characterizing and learning equivalence classes of causal dags under interventions. In *International Conference on Machine Learning*, pages 5541–5550. PMLR, 2018.
- Qiaoling Ye, Arash A Amini, and Qing Zhou. Distributed learning of generalized linear causal networks. *arXiv preprint arXiv:2201.09194*, 2022.
- Yue Yu, Jie Chen, Tian Gao, and Mo Yu. Dag-gnn: Dag structure learning with graph neural networks. In *International Conference on Machine Learning*, pages 7154–7163. PMLR, 2019.
- Xun Zheng, Bryon Aragam, Pradeep K Ravikumar, and Eric P Xing. Dags with no tears: Continuous optimization for structure learning. *Advances in neural information processing systems*, 31, 2018.

Federated Causal Discovery from Interventions (Supplementary Material)

Amin Abyaneh¹ Nino Scherrer² Patrick Schwab³ Stefan Bauer⁴ Bernhard Schölkopf⁵ Arash Mehrjou^{3,5,2}

¹Electrical and Computer Engineering Dept., McGill University, Montréal, Canada

²ETH Zürich, Zürich, Switzerland

³GlaxoSmithKline, Artificial Intelligence and Machine Learning, Zug, Switzerland

⁴TU Munich & Helmholtz AI, Munich, Germany

⁵Max Planck Institute for Intelligent Systems, Tübingen, Germany

A SUPPORTING EXPERIMENTS

We offer a thorough series of additional experiments utilizing the FedCDI framework, designed to rigorously assess its efficacy from diverse perspectives. These experiments encompass evaluations with both the random ER graphs outlined in the paper and structured DAGs commonly encountered in the literature.

Please note that throughout all experiments, the experimental criteria and metrics remain consistent with those outlined in the main paper, unless explicitly stated otherwise. We also use our proximity-based intervention aggregation method for all experiments, and the data generation mechanisms are the same for both ER and structured graphs.

A.1 PERFORMANCE OF FEDERATED ROUNDS

Figure 8 experiments demonstrate the way FedCDI performs after each *federated round*. These experiments are conducted for two different dataset sizes, and are a special case of Figure 2 in the main paper. The plots indicate the framework’s improvement at the end of each round (aggregation step), and the resulting final convergence after a few rounds.

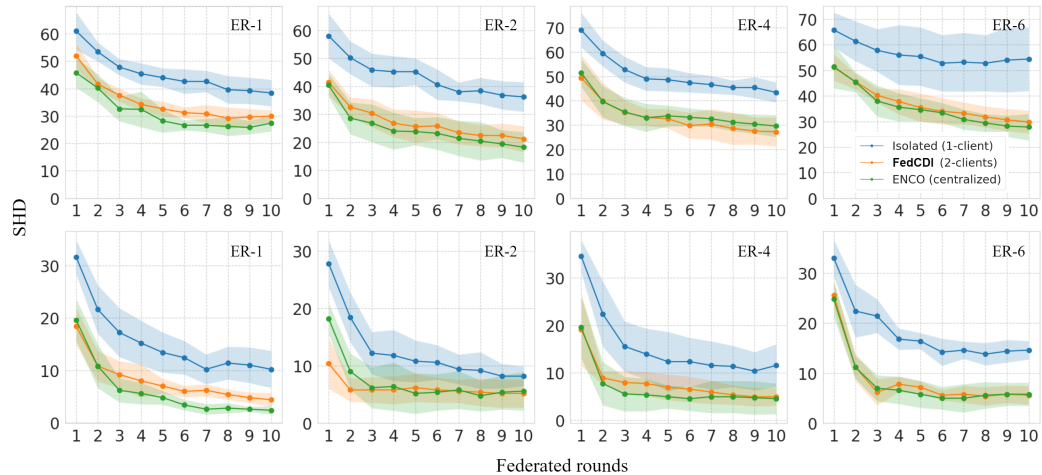


Figure 8: We provide a closer look into the gradual improvement at each federated round. Our method is compared against a centralized approach and an isolated client for two $D_{\mathcal{I}}$ sizes: 4 (first row) and 20 (second row). The centralized approach has access to the entire dataset, while each client in FedCDI and the isolated client all have access to half of the dataset. The plots demonstrate that FedCDI is closely following a centralized approach at each federated round.

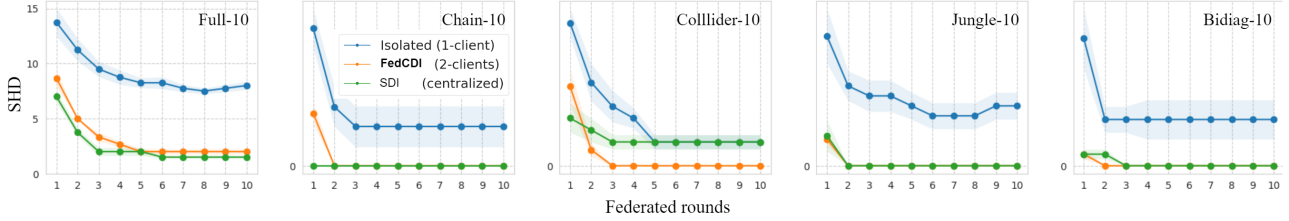


Figure 9: Evaluation of our approach when using SDI as the LCDM, instead of ENCO. We use structured graphs of size 10 here, and the improvement caused by the federated setup is still observable for all structured graph types. We need to reduce the graph size due to SDI’s computational time to achieve tractable experiments.

A.2 GENERALIZATION TO OTHER LCDM CANDIDATES

We believe that other continuous-optimization based structure discovery methods can be employed as the LCDM in our approach if modifications explained in our Methodology are applicable. For instance, in Figure 9, we switch the LCDM from ENCO to SDI [Ke et al., 2019], a work on causal discovery from observational and interventional samples. The SDI method is an iterative, score-based, continuous optimization strategy with three interconnected phases. Throughout these stages, both a functional representation of a set of independent causal processes and a structural representation of a DAG are trained simultaneously until convergence. Since the structural and functional parameters are interdependent, they undergo alternating stages of training. This alternation occurs between fitting the graph to observational data and scoring the graph on interventional samples, ultimately resulting in a belief about the underlying DAG.

Even when employing a federated setup, the results still demonstrate improvement upon replacing ENCO with SDI. It’s important to note that due to the significant computational demands of SDI, our experimentation is limited to structured graphs with 10 nodes. This computational challenge is why we primarily utilize ENCO in the main text and for most experiments. However, we anticipate that future advancements in implementation and integration of SDI into the federated setup could mitigate these complexities. Additionally, it’s worth mentioning that the underlying graphs for these experiments differ from the ER graphs introduced in the main text. Further details about the underlying data generator graphs for these experiments can be found in Appendix A.4.

A.3 ANALYSIS OF THE PREDICTION ENTROPY

Consensus, in the context of distributed systems, denotes the collective agreement among processes to converge on a specific value, typically attained through the voting mechanism of each process. This concept holds significant importance in federated learning. In this decentralized environment, achieving consensus ensures that all participating clients synchronize their contributions to the model update, resulting in a consistent and accurate global model. Consensus mechanisms play a crucial role in addressing the challenge of model divergence, where variations in local data and training conditions among clients can lead to divergent models. By attaining consensus, federated learning effectively mitigates the effects of data heterogeneity, ensuring that the aggregated model reflects a shared understanding of the data.

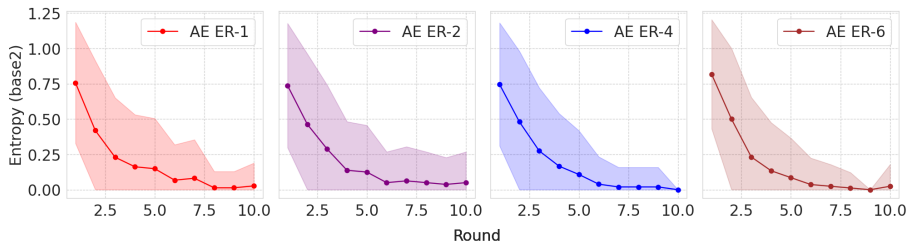


Figure 10: Average edge entropy for all the elements in the clients’ adjacency matrix for a 10-client federated setup is plotted here. The results reveal a substantial decrease in the values of edge entropy after each round, which serves as an empirical sign of convergence and indicates that the federated setup is progressing towards reaching a consensus among clients over the federated rounds. This result is critical to eliminate clients’ uncertainty about the global DAG.

In our study, we assess clients’ consensus through calculating the *average entropy* (AE) for each edge. This measure is

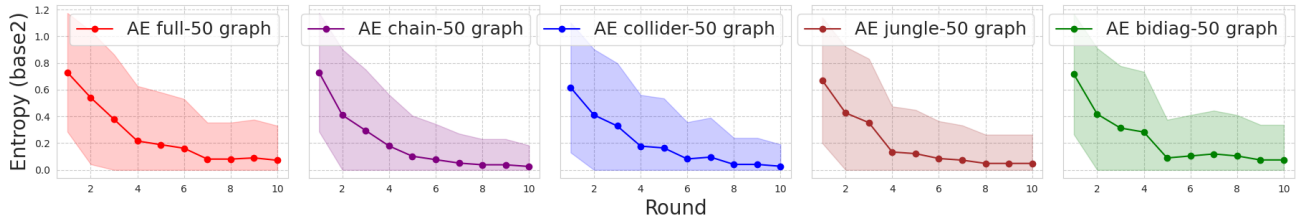


Figure 11: Average edge entropy for all the elements in the clients’ adjacency matrix for a 10-client federated setup plotted for structured graphs. The results reveal the same levels of decrease in the values of edge entropy after each round as Figure 10. The decreasing trend resembles the way clients with no access to close intervened covariates yield to the ones with more valuable knowledge over time.

based on the information exchanged between clients and the server at the end of each round. The empirical results depicted in Figure 10 and Figure 11 showcase the dynamics of average entropy reduction across different causal graphs as the rounds progress. Remarkably, our proposed approach demonstrates the ability to attain consensus in most cases within 10 rounds, although in certain scenarios, we observe a substantial reduction in average entropy without reaching complete consensus. These findings highlight the effectiveness of our approach in reducing uncertainty and aligning the distributed processes towards a shared belief about the global causal structure.

A.4 EXPERIMENTS ON STRUCTURED GRAPHS

We conduct further experiments on a range of structured graphs to further evaluate FedCDI. These graphs include the *chain*, *bidiag*, *full*, *collider*, and *jungle* graphs. In the *bidiag* graphs, the probability of a node X_i being connected to its immediate parents X_{i-1} and X_{i-2} is defined as $P(X_i = 1 | X_{i-1} = 1, X_{i-2} = 1)$. Similarly, the *chain* graph represents a simplified version, where the probability of a node X_i being connected to its immediate parent X_{i-1} is defined as $P(X_i = 1 | X_{i-1} = 1)$. Collider graphs involve a specific node X having all other nodes as its parents, with the probability of a node X_i being connected to its parents being $P(X_i = 1 | Pa(X_i))$. The *full* graph represents the densest connected graph possible, where the probability of a node X_i being connected to all preceding nodes X_1, X_2, \dots, X_{i-1} is defined as $P(X_i = 1 | X_1 = 1, X_2 = 1, \dots, X_{i-1} = 1)$. Lastly, the *jungle* graph introduces a binary tree structure with additional connections to a node’s parent’s parent. These experiments provide valuable insights into how our approach performs under different graph configurations, capturing diverse causal relationships and their complexities.

Figure 12 and Figure 13 show FedCDI performing consistently on datasets generated by structured graphs. Note that all the graphs here have the same size 20 as the random graphs, and the datasets are produced with the same process of Lippe et al. [2021] and Ke et al. [2019] with the same sizes as the main paper. The next plot, Figure 15, depicts the experimental results for vertical distribution of $D_{\mathcal{I}}$ where the underlying data generation process is built upon structured graphs, further verifying the results in the main paper.

B EXPERIMENT SETUP AND DETAILS

This section is dedicated to further details related to our experiments. These include the size and distribution of synthetic data, and a detailed algorithm for implementation of our proximity-based aggregation method.

B.1 DATASET SIZE AND DISTRIBUTION

For the entire experiments, aside from the baselining table, we use 10000 observational samples as $D_{\mathcal{O}}$ and 2000 samples for $D_{\mathcal{I}}$. For the baselining, however, we increase the size of $D_{\mathcal{O}}$, $D_{\mathcal{I}}$ to 25k and 5k to make the experiments compatible with other methods such as IGSP. These numbers correspond to the size of D , that is, the global dataset yet to be distributed among several clients. For example, in a 2-client setup, each client typically gets half of the observational data. Depending on the vertical or horizontal split of the interventional data, a client might get access to samples from all or part of dataset features. Samples of interventional data corresponding to a specific feature are further divided between clients if they share an intervened covariate. In scenarios where clients have access to disjoint covariates, the entire interventional samples corresponding to the intervened covariate is accessible to the client with access to interventions on that feature.

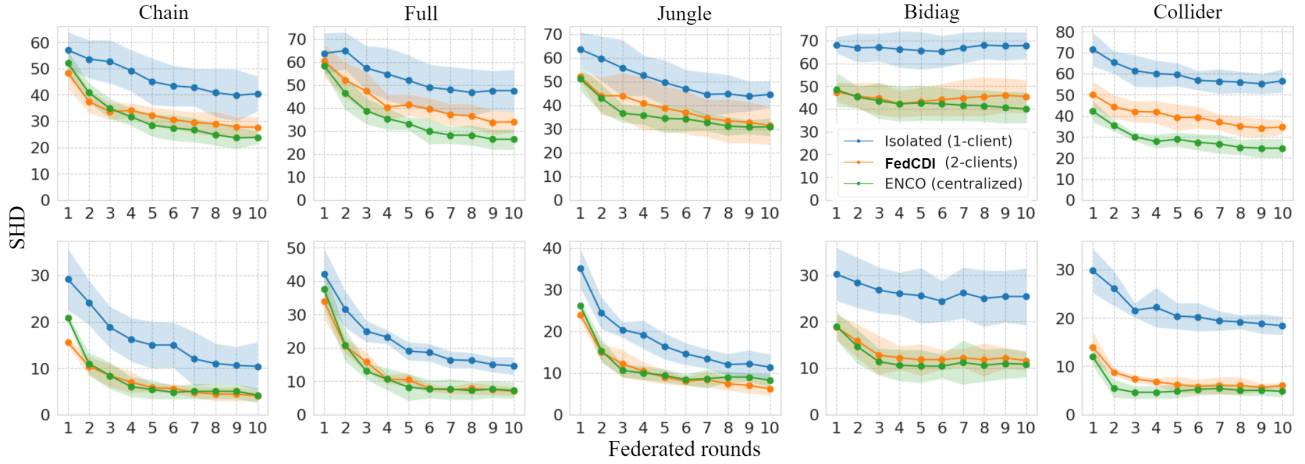


Figure 12: We provide a detailed analysis of the incremental improvement achieved in each federated round for *structured graphs*. Our method is compared against a centralized approach and an isolated client setting using two different sizes of $D_{\mathcal{I}}$: 4 (first row) and 20 (second row). In the centralized approach, the entire dataset is available, while in both FedCDI and the isolated client, each client has access to only half of the dataset. The plots clearly illustrate that FedCDI consistently tracks the performance of the centralized approach in every federated round.

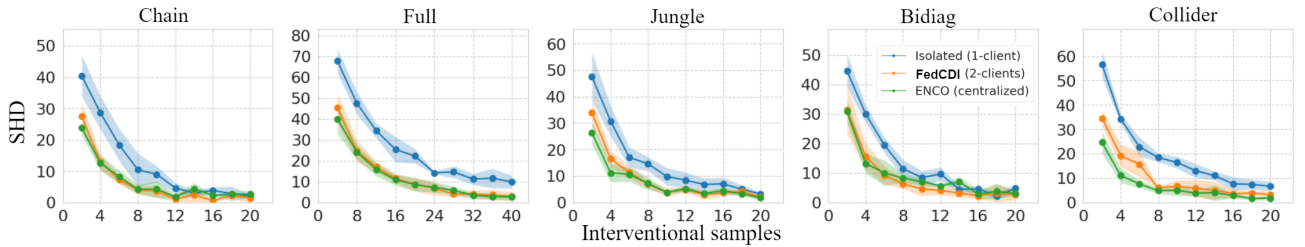


Figure 13: Our method is compared against a centralized approach and an isolated client based on the size of interventional data. The centralized approach has access to the entire dataset, while each client in FedCDI and the isolated client all have access to half of the dataset. The results of comparison to the centralized approach with structured graphs are aligned with that of the random ER graphs.

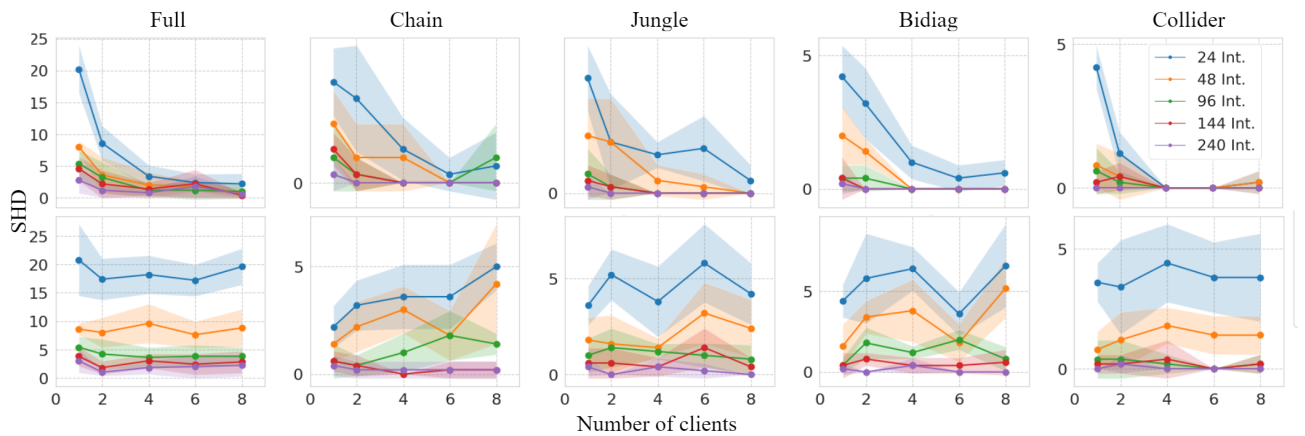


Figure 14: In the initial row, we witness the impact of involving more clients in FedCDI across varying sizes of $D_{\mathcal{I}}$. As the number of clients grows, the resulting DAG becomes more precise, correlating with the enlargement of $size(D_{\mathcal{I}})$. Unlike the first row, our approach effectively maintains knowledge as the fixed-size $D_{\mathcal{I}}$ is divided further among clients, where no new information added to the network with the advent of new clients.

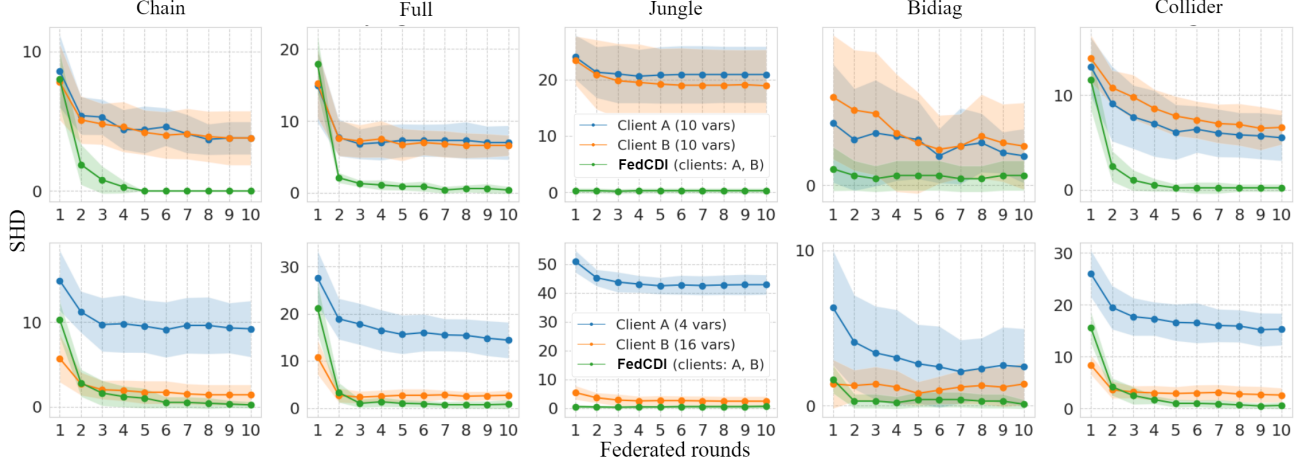


Figure 15: We compare three different setups with vertical distribution of $D_{\mathcal{I}}$, this time considering structured graphs. The setups are non-collaborative clients A and B with access to only a vertical subset of $D_{\mathcal{I}}$, and a federated setup where both clients collaborate through FedCDI. Evidently, FedCDI can take advantage of clients’ insight about the global structure, even from the less significant clients.

B.2 ALGORITHM FOR AGGREGATION METHOD

We provide a pseudocode for the proximity-based aggregation method in Algorithm 2. For further implementation details, please refer to the addressed code repository. Note that the `binary_step(ψ , $threshold = 0.5$)` just converts a belief about the adjacency matrix into an standard adjacency matrix using a binary step function. The more complex of undefined functions is `get_path_beliefs`, that retrieves the beliefs for all possible paths between the intervened covariate to the disputed edge within the DAG, based on the most updated global knowledge.

Algorithm 2 Proximity-based federated aggregation method from interventional data.

```

function proximity_based_aggregation( $\psi$ ,  $\{\psi^1, \dots, \psi^k\}$ )
   $adj\_mat \leftarrow \text{binary\_step}(\psi, \text{threshold} = 0.5)$ 
  for  $X_i \rightarrow X_j$  in edges( $adj\_mat$ ) do
    for  $k = 1$  to  $K$  do
      for  $X_s$  in  $X_{C_k}^{\mathcal{I}}$  do
         $\psi_{sp}^k, \dots, \psi_{ij}^k \leftarrow \text{get\_path\_beliefs}(X_s, X_i \rightarrow X_j)$ 
         $r_{ij}^k \leftarrow \max(\psi_{sp}^k \cdot \dots \cdot \psi_{ij}^k \cdot m_s^k, r_{ij}^k)$ 
      end for
       $\hat{r}_{ij}^k = e^{\beta r_{ij}^k} / \sum_{k \in [K]} e^{\beta r_{ij}^k}$ 
    end for
     $\psi_{ij}^* = \sum_{k \in [K]} \hat{r}_{ij}^k \psi_{ij}^k$ 
  end for
  return  $\psi^*$ 

```

▷ latest structure from previous round’s ψ

▷ calculate reliability scores

▷ retrieves beliefs for all paths: $X_s \rightarrow X_p \rightarrow \dots \rightarrow X_i \rightarrow X_j$

▷ over paths like $X_s \rightarrow \dots X_j \rightarrow X_i$

▷ reliability scores to probabilities

▷ final aggregation

B.3 GRAPH AND DATASET GENERATION

We adhere to the random Erdős–Rényi [Erdős and Rényi, 2011] model to generate experimental DAGs of size $d = 20$. Erdős–Rényi graphs, named after mathematicians Paul Erdős and Alfréd Rényi, are a type of random graph model that

provides a simple and fundamental framework for studying random network structures. These graphs are characterized by their random and independent edge formation. Each edge is added with an independent pre-determined probability from the others, and is modeled by $G(d = 20, p)$. Hence, each edge is included in the graph with probability p . The probability for generating a graph that has d nodes and n edges is $p^n(1 - p)^{\binom{n}{2}}$.

Our experiments are conducted for $ER - n$ graphs where $n \in \{1, 2, 4, 6\}$. The value of $m = n.d$ (where n is the parameter in $ER - n$) is equal to the expected number of edges. For example, as $d = 20$ throughout the experiments, an $ER - 2$ DAG has an expected number of $m = 40$ edges. Further, to determine the orientation of the edges, we assume the causal ordering of (X_i, X_j) to be oriented $X_i \rightarrow X_j$ if $i < j$, otherwise $X_j \rightarrow X_i$.

Same as Lippe et al. [2021] and Ke et al. [2019], we employ categorical variables of 10 categories each. The process utilizes randomly initialized neural networks – MLPs with two layers with categorical inputs – to model the ground-truth conditional distributions. For instance, when a variable X_i has M parents, M embedding vectors are stacked and passed as an input. The hidden size of the layers is 48, and their architecture uses a LeakyReLU activation functions between layers and a softmax activation to find a distribution for the output. More information about the process could be found in the appendix of Lippe et al. [2021].

B.4 BASELINES IMPLEMENTATION

We use standard GitHub implementations of baselines in all cases. Aside from the size of the observational and interventional data required for our experiments, we keep other parameters of these models the same as their default values. Causal discovery toolbox [Kalinathan et al., 2020] is the only third-party library that we use, others are all developed by the original implementations of the corresponding authors. Table 2 presents a list of open source implementations used in our experiments with other baselines in the literature.

Table 2: Baselines used in this work and the corresponding code repositories

Method	Code
ENCO	https://github.com/phlippe/ENCO
IGSP & GIES	https://github.com/FenTechSolutions/CausalDiscoveryToolbox
SDI	https://github.com/nke001/causal_learning_unknown_interventions
NOTEARS-ADMM	https://github.com/ignavierng/notears-admm
FedDAG	https://github.com/ErdunGAO/FedDAG

B.5 HYPERPARAMETERS

As appears in our methodology, there are a number of hyperparameters in our work that need further tuning. We mostly employ grid search for hyper parameter optimization. Note that for the initial mass, the value itself is not of critical importance. The importance lies in the difference between the injected mass for different clients when compared to each other. Therefore, we suggest setting the initial mass based on the size of interventional data for each client, and normalize this number across all clients between 0 and 1. We have tried setting the initial mass according to both interventional and observational data as well, and it can work better in some setups, especially if the size of observational data is critically low. Otherwise, the effect of choosing the mass based on observational samples becomes insignificant.

Table 3: Hyperparameters and Their Effects

Hyperparameter	Description	Plausible value(s)
λ_{prior}	Controlling the effect of prior belief on LCDMs local optimization	0.01 - 0.1
m_i^k	The initial mass of clients for the aggregation.	$\propto \frac{D_{T^k}}{D_I}, 0 \leq m_i^k \leq 1$
β	The softmax parameter for calculation of reliability scores.	0.15